

# Localized Hydrogen in Titanium Welds

*Ion microprobe analysis of titanium EB welds showed that hydrogen can play a significant role in massive void formation*

BY P. N. ADLER, J. KENNEDY AND F. G. SATKIEWICZ

**ABSTRACT.** Ion microprobe analysis was utilized to investigate the role of hydrogen in the formation of massive voids during electron beam welding of titanium and to evaluate hydrogen

contamination and its removal associated with vacuum and air annealing. Localized measurements of hydrogen concentration were made on hydrogen charged and annealed

surfaces as well as on simulated void specimens that were prepared by hydrogen charging and welding. Hydrogen enrichment was observed near massive voids, which indicates that hydrogen does play a significant role in the formation of voids in hydrogen-charged specimens. Vacuum annealing was most effective in reducing the hydrogen concentration, whereas air annealing caused significant increases.

## Introduction

An investigation of the causes and nature of unusual weld imperfections — so-called “massive voids” — began after they were detected radiographically in 2-in. thick electron beam welded Ti-6Al-4V. These internal voids in the weld metal can be generally described as thin and irregular, with their longest dimension oriented in the vertical plane of the weld. Massive void defects, when simulated by hydrogen charging and electron beam welding, have appeared either as isolated flaws or in the relatively orderly array shown by Fig. 1. Compared to other types of weld defects, massive voids bear a similarity to wormhole formations that sometimes appear in steel weld metal at the solidification interface as a result of CO gas evolution.<sup>1</sup>

One possible cause of massive void formation is hydrogen entrapment during welding. Hydrogen contamination has been reported to contribute to voids in aluminum welds<sup>2</sup> and in titanium welds.<sup>3-5</sup> Sources for introducing hydrogen are numerous during materials preparation prior to welding; hydrogen is also present as a result of its solid solubility in both the

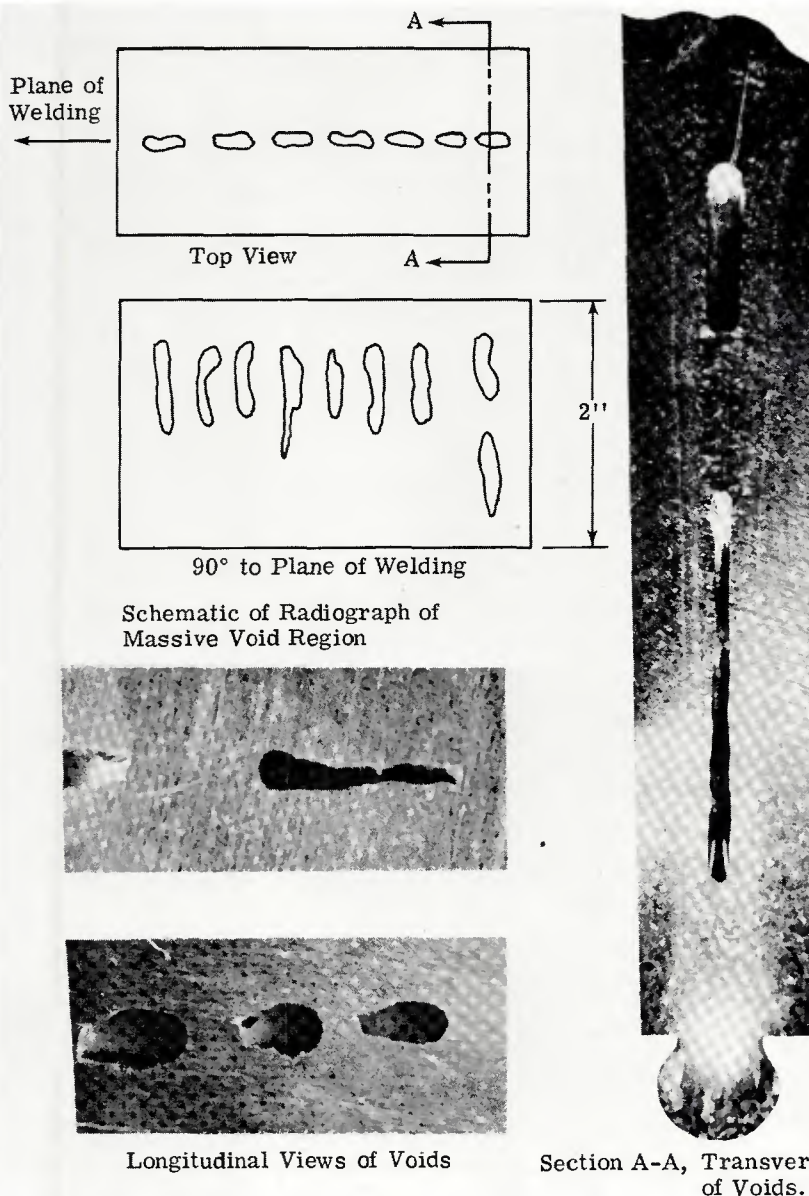


Fig. 1 — Simulated massive voids in 2-in. thick Ti-6Al-4V after hydrogen charging and electron beam welding

P. N. ADLER and J. KENNEDY are with the Materials Research Group, Grumman Aerospace Corp., Bethpage, New York and F. G. SATKIEWICZ is with GCA Corp., Bedford, Mass.

$\alpha$  and  $\beta$  phases of titanium.

The present investigation was initiated to clarify the role of hydrogen in the massive void problem and to evaluate the effect of various treatments on hydrogen contamination and its elimination. While it is clear that hydrogen could be of significance to the void problem, other factors related to the welding process, such as joint fit-up, may be contributing or primarily responsible. Evaluation of welding factors, however, was not within the scope of this investigation.

The analysis in this paper was performed on hydrogen-charged, electron beam welded specimens that simulated the actual production massive void defects. To determine the presence of hydrogen, localized concentration measurements are needed since bulk analysis is not indicative of the concentration at the areas of primary interest, such as the void surfaces and adjacent regions shown in Fig. 1.

Means of determining localized hydrogen concentrations are limited and, for the most part, still in a developmental stage. One approach, the Lithium Nuclear Microprobe,<sup>5</sup> has the capability of determining hydrogen concentration profiles to a depth of approximately  $5 \mu\text{m}$  ( $0.2 \times 10^{-3}$  in.) in  $0.1 \mu\text{m}$  ( $4 \times 10^{-6}$  in.) increments. This technique was capable of discerning both hydrogen depletion and enrichment at the surface of hydrogen-in-titanium NBS Standards<sup>7</sup> and would be applicable to the present study; however, an appropriate particle accelerator facility was not readily available at the time evaluation was necessary.

Other approaches for measuring localized hydrogen concentrations include autoradiographic techniques,<sup>6</sup> use of a neodymium film,<sup>9</sup> a laser microprobe technique,<sup>10</sup> and an ion microprobe technique.<sup>11</sup> Of these, the ion microprobe approach appeared the most appropriate for our purpose because of its reported technical capability and availability. This paper describes localized hydrogen concentration measurements made using sputter ion source mass spectrometry, commonly referred to as the ion microprobe approach. Samples were examined to calibrate the ion microprobe and to evaluate conditions of interest to the incidence and repair of voids.

## Experimental Procedure

### Ion Microprobe Approach

Measurements were made by using a GCA IMS-101B ion microprobe analytical mass spectrometer. Essentially, the operation consists of sputtering the sample surface and

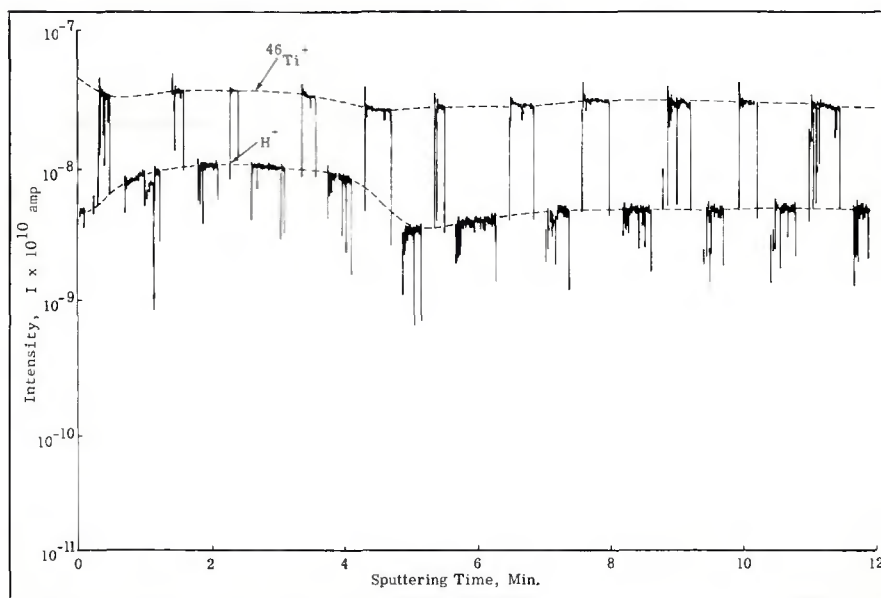


Fig. 2 — Typical ion intensity output data for  $\text{H}^+$  and  $^{46}\text{Ti}^+$  as a function of sputtering time for electron beam welded sample at void area (A6-1). Interpolation between monitoring times indicated by dashed lines

measuring the resulting ion output with a mass spectrometer. The sample is mounted on an appropriate holder and placed in a vacuum chamber. A beam of argon ions (other ions may also be used) is focused on the sample, thereby sputtering the surface. The sputtered ions pass into a secondary ion optics system which contains a double focusing mass spectrometer. Ions are filtered according to mass and energy and are detected by an ion multiplier. Typically, the atomic or polyatomic output spectra are plotted to determine the ion species that are present, or the intensity output of a particular ion species is monitored as a function of sputtering time. Detailed descriptions of this approach are available.<sup>11-13</sup>

The sputtering procedure is of primary importance to sampling and, thereby, to the nature of the localized measurement. Either a focused or a defocused ion sputtering beam can be used. The focused beam results in a more localized areal sampling and a higher average penetration rate. The major portion of our work was done using a focused beam with an average penetration rate of  $2.5 \mu\text{m}/\text{min}$  ( $0.1 \times 10^{-3}$  in./min). This produced a "teardrop" shaped cratered surface of about  $1.4 \text{ mm}$  ( $0.056$  in.)  $\times$   $0.6 \text{ mm}$  ( $0.024$  in.). Use of a defocused sputtering beam results in a lower penetration rate, of the order of  $0.025 \mu\text{m}/\text{min}$  ( $0.001 \times 10^{-3}$  in./min), and in a flat crater.

To determine the hydrogen concentration, the output intensity of  $\text{H}^+$  was normalized to that of  $^{46}\text{Ti}^+$ . This simplifies calibration and allows for

equipment and sample fluctuations. Typical ion intensity output data of  $\text{H}^+$  and  $^{46}\text{Ti}^+$  for a sample of Ti-6Al-4V at a void region are shown in Fig. 2, where output intensity is plotted as a function of sputtering time. Output of only one ion at a time could be scanned so that normal practice in evaluating these data was to interpolate during intermediate periods. The ratio of the output intensity of  $\text{H}^+$  to  $^{46}\text{Ti}^+$ , subsequently designated R, is a measure of the hydrogen concentration. Actual hydrogen concentrations were determined by calibrating R values with the known concentration of samples.

The data shown in Fig. 2 do not represent the actual hydrogen concentration depth profile, since sputtering time is not a direct measure of sampling depth. During sputtering, ions evolve from the entire three dimensional crater surface so that sputtering time is actually indicative of some average sampling depth. However, since the maximum crater depth increases at a reasonably linear rate ( $2.5 \mu\text{m}/\text{min}$  for the focused sputtering conditions generally used in this work), some approximation to the existing profile can be made by considering the over-all concentration change as a function of maximum crater depth. Such a profile is not as well resolved as the actual concentration-depth profile, but it is indicative of the existing concentration as well as of the extent of concentration gradients. In subsequent reporting of results, both sputtering time and maximum crater depth will be indicated to differentiate the sputtered profile from the actual con-

centration-depth profile.

### Samples Examined

1. *Samples for Calibration.* Initially, three hydrogen-in-titanium standards from the National Bureau of Standards were examined. These were pure  $\alpha$ -Ti standards that had been previously studied.<sup>6,7</sup> A sample of Ti-5Al-2.5 Sn sheet, 1 mm (0.040 in.) thick, containing a lower bulk hydrogen concentration than the NBS standards, was also used for calibration.

2. *Samples Related to the Massive Void Problem.* Samples of Ti-6Al-4V representing various conditions of interest to the incidence and repair of voids were studied. Specific material conditions were as follows: (1) as-received (mill annealed); (2) hydrogen-charged; (3) hydrogen-charged and electron beam welded (containing voids); (4) hydrogen-charged and vacuum-annealed at 704 C (1300 F) for 3 and 24 hr; (5) hydrogen-charged, electron beam welded (containing voids), and vacuum-annealed at 704 C (1300 F) for 24 hr; (6) hydrogen-charged and air annealed at 704 C (1300 F) for 3 and 24 hr.

Hydrogen charging consisted of cathodic charging for one hour in a five percent sulfuric acid bath at initial conditions of 9V and 5A/in.<sup>2</sup> The air-annealed samples received an alkaline soap clean and a "Turco T-50" coat prior to annealing and were salt-bath dipped and acid pickled to remove a minimum of  $38 \mu\text{m}$  ( $1.5 \times 10^{-3}$  in.) of surface subsequent to annealing. Vacuum-annealed samples did not receive any pickling prior or subsequent to annealing; vacuums were of the order of  $10^{-5}$  to  $10^{-6}$  mmHg. Hydrogen-charged and electron beam welded samples were acid pickled prior to welding to remove  $2.5 \mu\text{m}$  ( $0.1 \times 10^{-3}$  in.) of surface.

All samples were final cut to accommodate the sample holder of the ion microprobe; a cutoff wheel cooled by water containing a soluble oil was used. Maximum sample size was 6 mm (0.240 in.) thickness  $\times$  12 mm (0.480 in.) width  $\times$  32 mm (1.28 in.) length; most of the samples were approximately 6 mm (0.240 in.) long to make possible examination of about four samples on each evacuation of the sample chamber of the ion microprobe. Samples were cleaned following cutting with a trichloroethane solvent in an ultrasonic bath and received final rinsing with Freon "TF." Bulk hydrogen concentration was also determined for each sample by vacuum fusion analysis.

Two general types of surfaces were examined: "as prepared" surface conditions, e.g., hydrogen-charged surface; and surfaces that were cut.

This latter procedure was necessary for examination of internal voids and to determine concentrations within the bulk. These two sampling conditions are illustrated in Fig. 3. Sputtering profiles obtained on cut surfaces are hereafter designated as bulk profiles.

## Results and Discussion

### Samples for Calibration

Analysis of the atomic and polyatomic spectra at the surface of one hydrogen-in-titanium standard, NBS 352, was made with a defocused sputtering beam. These spectra showed the presence of chloride ions in addition to the normally expected species. No other unusual elements were present. The chloride may be a result of the cleaning procedure used by NBS in sample preparation, or a residual of the titanium extraction process involving reduction of  $\text{TiCl}_4$ . In any case, although the presence of chloride was not considered significant to our investigation, its detection was indicative of the capability of the approach.

Relative hydrogen concentration, R, as a function of sputtering time for three different NBS standards and the Ti-5Al-2.5Sn sheet sample is shown in Fig. 4 where each curve represents a specific sputtered spot. As discussed previously, R is the ratio of the output intensity of  $\text{H}^+$  normalized to that of  $^{46}\text{Ti}^+$ . Crater depth, also indicated in Fig. 4, is based on an average  $2.5 \mu\text{m}/\text{min}$  removal rate. The general values for R shown in Fig. 4 are consistent with the bulk hydrogen concentrations of these samples.

Using the R values for deepest penetration, we find a linear relationship between R and bulk hydrogen concentrations to about 100 ppm, as shown in Fig. 5. For the highest concentration standard, NBS 354, there is a divergence from linearity. This sample was previously shown to be depleted of titanium hydride to a depth of approximately  $50 \mu\text{m}$  ( $2 \times 10^{-3}$  in.) (Ref. 7). Therefore, the apparent low value of R may be a result of the surface-dominated sampling obtained by sputtering.

However, it is also possible that there is reduced ionizability of  $\text{H}^+$  when hydrogen is bonded as titanium hydride rather than as an interstitial element in the solid solution of titanium. A great deal of the hydrogen in the NBS 354 sample, probably more than half of the bulk concentration, should exist in the form of titanium hydride. Additional evaluation would be required to resolve whether the divergence from linearity above 100 ppm in Fig. 5 is real; fortunately, the values of R encountered

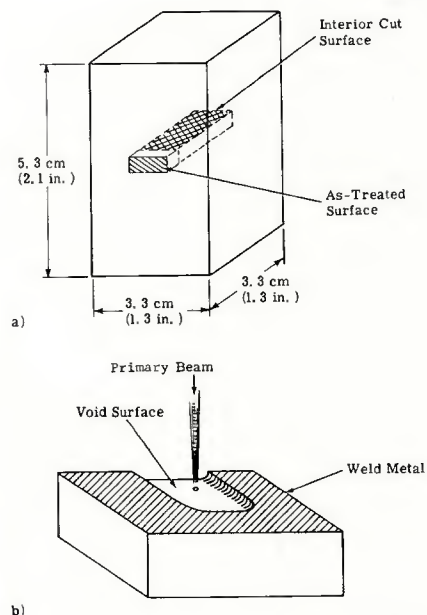


Fig. 3 — Typical sampling for Ti-6Al-4V material related to massive void problem. (a) Both "as-treated" and cut surfaces were sputtered. Profiles sputtered from cut surfaces are designated as bulk profiles. (b) Schematic of sputtering beam focused directly on void surface

in this work were generally within the linear portion of this relationship.

To establish a more valid calibration than that based on only three samples, the R values measured at maximum depth of penetration for all samples tested were also considered. These values, along with those of Fig. 5, are shown in Fig. 6. The concentrations indicated in subsequent profiles are based on a least-squares fit of the data of Fig. 6.

### Samples of Ti-6Al-4V Related to the Massive Void Problem

Atomic spectra were evaluated for almost half of the samples examined. In no case was any unusual ion species observed.

1. *As-Received and Hydrogen-Charged Samples.* Hydrogen concentration-sputtering time profiles for typical "as-received" material as well as for hydrogen-charged samples are shown in Fig. 7. Sample 43 (hydrogen-charged) was pickled subsequent to charging to remove approximately  $2.5 \mu\text{m}$  ( $0.1 \times 10^{-3}$  in.) of surface. As indicated in Fig. 7, hydrogen charging appears to increase the surface hydrogen concentration over that of as-received material, but for two of the five hydrogen-charged areas sputtered, no increase is observable.

To evaluate the effect of hydrogen charging on the concentration within the bulk, three spots were sputtered on a surface cut to expose interior material (see Fig. 3a). The spots were

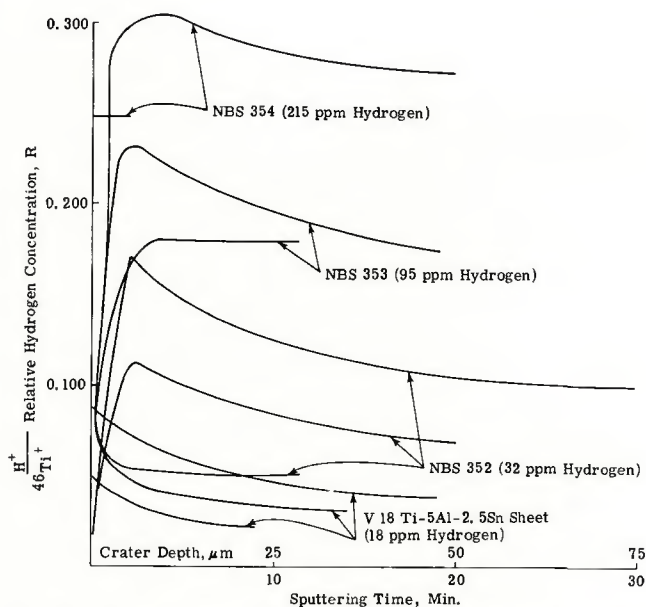


Fig. 4 — Relative hydrogen concentration,  $R$ , ( $H^+/^{46}Ti^+$ ) as a function of sputtering time for calibration samples. Vacuum fusion bulk analyses are also indicated

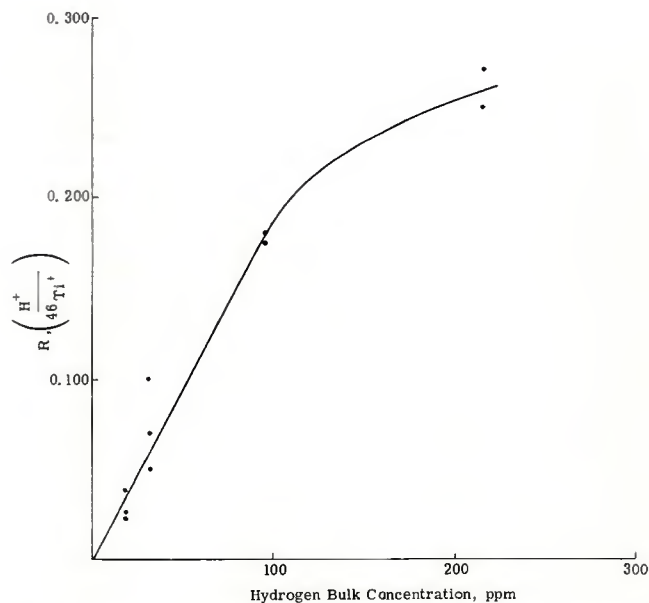


Fig. 5 — Relationship between the relative hydrogen concentration,  $R$ , and bulk analysis for calibration samples

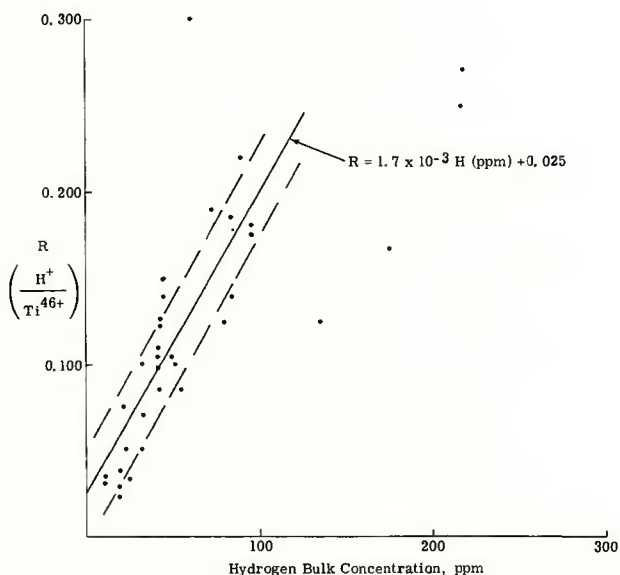


Fig. 6 — Calibration for relative hydrogen concentration,  $R$ , based on the samples herein reported. A least-squares fit of the data, based on most of the points, as well as the standard error range is indicated

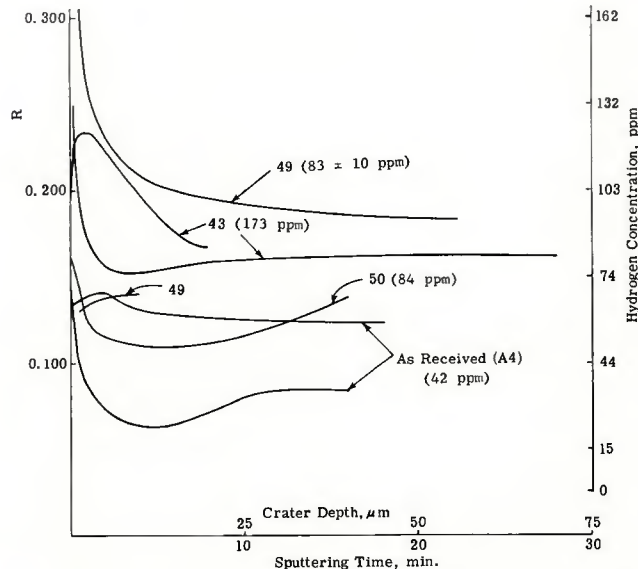


Fig. 7 — Concentration-sputtering time profiles for as-received and hydrogen-charged samples of Ti-6Al-4V. Sample designation and bulk hydrogen analysis are included.

roughly 1.6 mm (0.063 in.), 4.7 mm (0.188 in.), and 7.8 mm (0.313 in.) from the "as-charged" surface of Sample 50. The concentration-sputtering time results for these bulk profiles are shown in Fig. 8. The high concentration of hydrogen at the cut surface for the two areas closest to the originally charged surface is difficult to understand since high concentrations were not observed on the charged surface (see Sample 50 in Fig. 7). There is also a systematic decreasing trend in the hydrogen concentration with increasing distance from the charged surface, sug-

gesting that the extent of hydrogen penetration during charging may be significant to a depth of at least 4.7 mm (0.188 in.). From the results shown in Figs. 7 and 8, hydrogen charging appears to be an effective but inconsistent means of introducing hydrogen.

2. *Hydrogen-Charged and Electron Beam Welded with Voids.* Two samples containing voids, A6 and A6-1, were examined to evaluate the extent of hydrogen segregation in the void area. These samples were cut so that the sputtering beam could be focused directly on the void, as shown

in Fig. 3b. Concentration-sputtering time profiles adjacent to and on void areas are shown in Fig. 9.

To estimate the hydrogen concentrations for the high  $R$  values of these samples, it was necessary to extrapolate the least-square fit in Fig. 6 beyond its present range of validity. This appears to be a reasonable procedure since the hydrogen in these  $\alpha + \beta$  phase samples is in solid solution rather than in the form of hydride and would be expected to have an ionizability comparable to that in the  $\alpha$  phase alone. In addition, this approximation is a conservative one since it

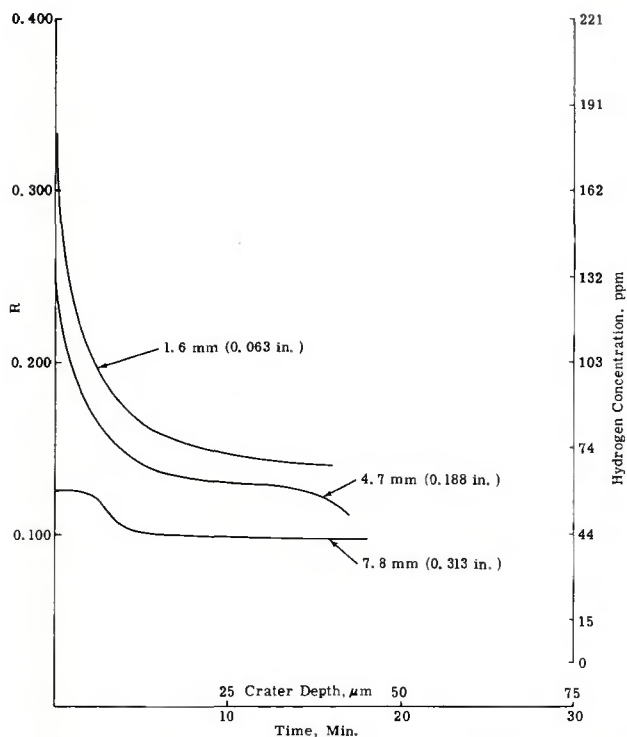


Fig. 8 — Concentration-sputtering time bulk profiles from interior of hydrogen-charged Ti-6Al-4V (Sample 50). Distances from as-charged surface as indicated

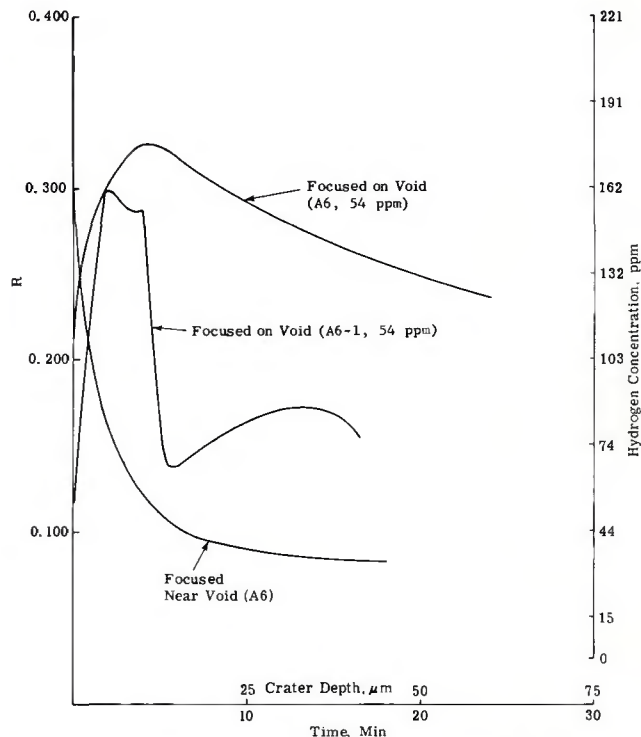


Fig. 9 — Concentration-sputtering time bulk profiles at void regions in hydrogen-charged and electron beam welded samples of Ti-6Al-4V (A6 and A6-1)

would tend to underestimate the existing hydrogen concentration obtained by using Fig. 5.

As can be observed in Fig. 9, high hydrogen concentrations are associated with void areas. For the sputtered area near a void, the hydrogen concentration is much lower. There is some possibility that the high hydrogen concentrations are an experimental artifact related to sputtering the surface of a void, but the unusual character of the profile of A6-1 suggests that hydrogen has localized near the void. This localized condition would not be identifiable by bulk analysis.

**3. Hydrogen-Charged and Vacuum-Annealed at 704 C (1300 F).** The concentration-sputtering time profiles for hydrogen-charged samples that were subsequently vacuum-annealed are shown in Fig. 10. After only 3 hr of vacuum annealing at 704 C (1300 F) and  $10^{-5}$  to  $10^{-6}$  mmHg, the surface hydrogen concentration is reduced to about 15 ppm. Annealing for 24 hr reduces the concentration to about 3 ppm. This is in excellent agreement with an expected concentration of 1 ppm based on equilibrium of  $\alpha$ -Ti at 700 C with a hydrogen partial pressure at  $10^{-5}$  to  $10^{-6}$  mmHg (Ref. 14).

To evaluate the effect of annealing time on the diffusion of hydrogen from the interior of the sample, bulk profiles were measured after both 3 and 24 hr of vacuum heating. Areas

sputtered were from 3.1 mm (0.125 in.) to 18.6 mm (0.750 in.) from the evacuated surface. After 3 hr of annealing, the hydrogen concentration near the evacuated surface is much lower than that in the bulk. Use of a 24-hr vacuum anneal substantially reduces the concentration for all depths examined. Although these data are too limited to determine the diffusivity,  $D$ , in this alloy, they can be used to evaluate the validity of simplifying assumptions made for diffusion calculations.

The concentration profiles following 3 and 24-hr vacuum annealing at 704 C (1300 F) have been calculated by considering diffusion of hydrogen from a sphere of radius 2.5 cm (1 in.). These profiles, shown in Fig. 11, are based on the limiting boundary conditions of constant surface concentration and constant diffusivity,<sup>15</sup> and the reported hydrogen diffusivities in  $\alpha$  and  $\beta$  phases.<sup>16</sup> Ion microprobe results after 3 and 24-hr vacuum annealing, taken from data at maximum penetration, are also shown in Fig. 13. Actual diffusion was from an approximate 3.3 cm (1.3 in.)  $\times$  3.3 cm (1.3 in.)  $\times$  5.3 cm (2.1 in.) block. For the 3-hr anneal, there is close agreement between the ion microprobe results and calculated diffusion in the  $\beta$  phase. After 24 hr, calculated diffusion in  $\alpha$ -titanium fits the ion microprobe results. Initially, it appears that diffusion in the  $\beta$  phase is controlling whereas at lower con-

centrations and longer times, diffusion in the  $\alpha$ -phase is limiting. The agreement between actual and calculated results is quite good and shows the applicability of an analytic approach in future considerations.

As was expected, vacuum annealing also serves to eliminate hydrogen from interior void areas. After vacuum annealing for 24 hr, the concentration-sputtering time bulk profile at the void indicated a hydrogen concentration below 10 ppm.

**4. Hydrogen-Charged and Air-Annealed at 704 C (1300 F).** Concentration-sputtering time profiles for hydrogen-charged samples that were subsequently air annealed are shown in Fig. 12. Although there is wide variation in the results, exposure in air at this temperature appears to increase the surface hydrogen concentration. This increase is expected from equilibrium considerations for the initial concentration of this sample (roughly 51-133 ppm).

If ideal gas conditions are assumed, the partial pressure of hydrogen in the air can be approximated as  $10^{-1}$  mmHg (Ref. 17). At 704 C (1300 F), the concentration of hydrogen in  $\alpha$ -Ti in equilibrium with this partial pressure of hydrogen gas would be 100-150 ppm (Ref. 14). Therefore, samples with lower concentrations should absorb hydrogen, whereas samples of higher concentration should outgas hydrogen. The wide variation in air-annealed results may

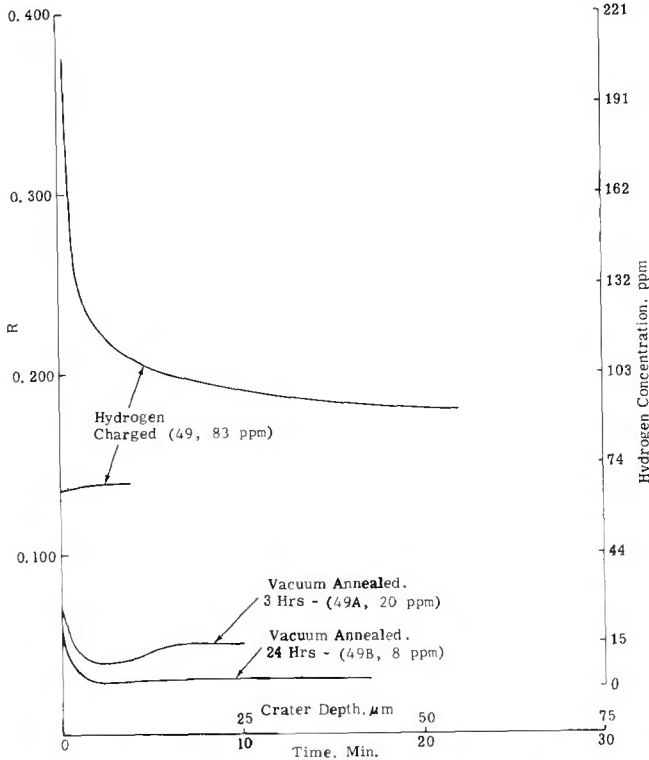


Fig. 10 — Concentration-sputtering time profiles for hydrogen-charged and charged and vacuum-annealed samples. Annealing for times indicated at 704 C (1300 F) at  $10^{-5}$  to  $10^{-6}$  mmHg

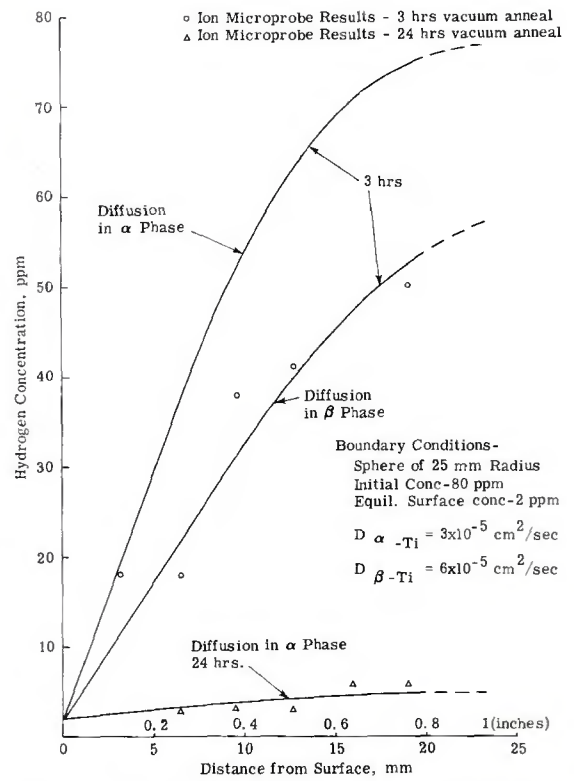


Fig. 11 — Calculated hydrogen-diffusion profiles compared with ion microprobe bulk profile results in 49A and 49B samples. Calculation based on diffusion from a sphere at 704 C (1300 F) at  $10^{-5}$  mmHg partial pressure of hydrogen. Diffusion in both  $\alpha$  and  $\beta$  phases of titanium is considered

be related to the nonuniformity associated with the prior hydrogen charging treatment that was previously discussed.

**Profile and Over-all Concentration Evaluation**

A graphical summary of the ion microprobe analyses for the various treatments examined is shown in Fig. 13. The values represent the average hydrogen concentration over a thickness from 5  $\mu$ m (approximately  $0.2 \times 10^{-3}$  in.) below the surface to an average sputtering depth of 39  $\mu$ m (approximately  $1.5 \times 10^{-3}$  in.). An initial depth of 5  $\mu$ m after the first 2 minutes of sputtering was selected as the starting point because of difficulty in characterizing the initial sputtering data. For many of the samples examined, the concentration-sputtering depth profile decreases sharply during the first two minutes.

It is unclear at this time whether this represents a real concentration effect or an experimental artifact associated with sample preparation or sputtering physics. In most cases where a particular spot was resputtered after being held in the evacuated sputtering chamber, the same decrease originally observed was again encountered. On the other

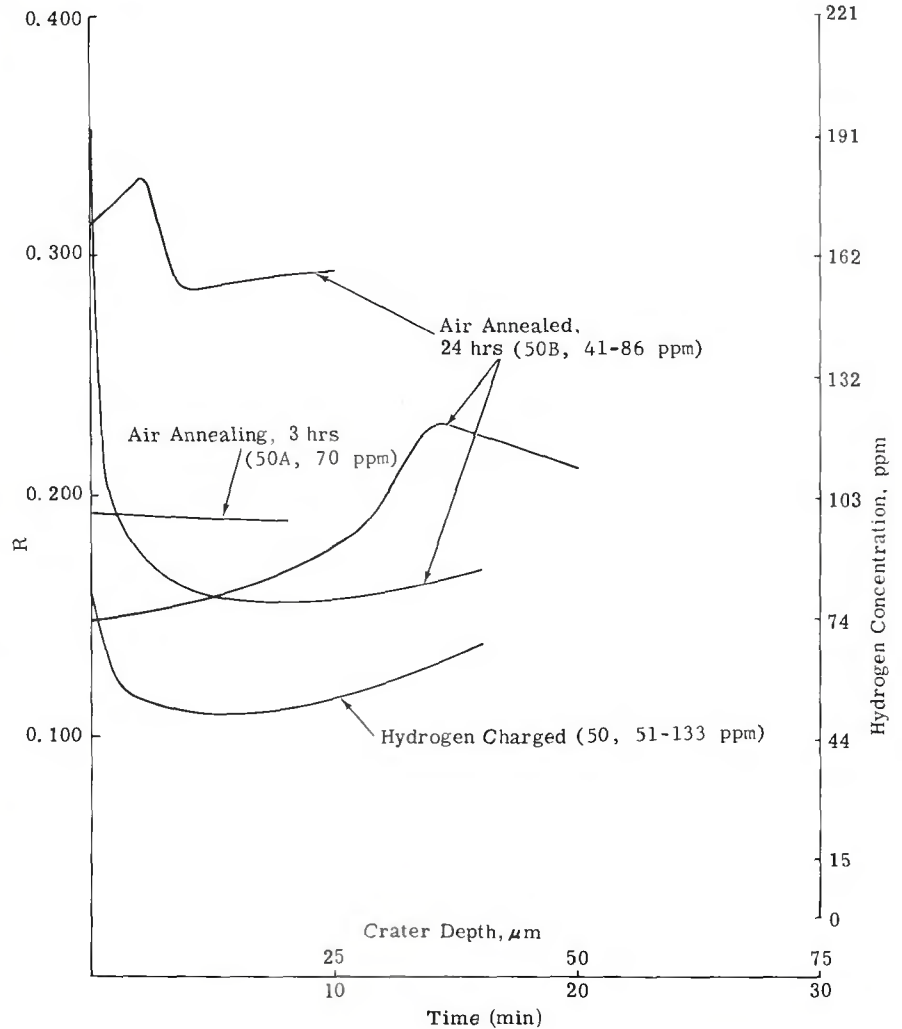


Fig. 12 — Concentration-sputtering time profiles for hydrogen-charged and charged and air-annealed samples. Air annealing at 704 C (1300 F) for 3 and 24 hr

hand, there appears to be a decrease in hydrogen concentration near the surface for some samples, particularly the NBS standards (see Fig. 4).

To evaluate the initial surface concentration, attempts were made to utilize a defocused sputtering beam at the slower sputtering rate of 0.025  $\mu\text{m}/\text{min}$  ( $0.001 \times 10^{-3} \text{ in.}/\text{min}$ ). However, significant concentration differences between samples could not be discerned using this approach. It was suspected that preparation residuals or hydrogen adsorption during sputtering was overshadowing the existing concentration. Because of time limitations, the defocused beam approach was limited to atomic spectra analysis. Additional study would be required to evaluate fully the applicability of this approach for hydrogen analysis within the first few microns of sample surface.

Although the hydrogen concentration during initial sputtering may be difficult to define, there appears to be good correlation with the results for deeper penetration (approximately 5  $\mu\text{m}$  and beyond) and bulk analysis (see Fig. 6). There is also consistency with the expected concentration levels resulting from different processing treatments (see Fig. 13). As indicated in Fig. 13, hydrogen concentration increased as a result of hydrogen charging as well as air annealing, and dramatically decreased after vacuum annealing. A high hydrogen content was indicated for the void surface in an electron beam weld, but was effectively decreased by vacuum annealing.

## Conclusions

Results of sputter source ion microprobe analysis of the titanium samples herein reported indicate the following:

1. The hydrogen concentration near the surface for different samples was found to be consistent with sample history. This approach appears to be applicable to analysis of hydrogen near titanium surfaces. Concentrations within the first few microns were not definable from the current effort.

2. Localized hydrogen enrichment was observed in the vicinity of voids prepared by hydrogen charging and electron beam welding. Such enrichment indicates that hydrogen plays a role in the formation of voids prepared with hydrogen-charged surfaces. It is not certain, however, that voids produced without hydrogen charging are similarly hydrogen-related.

3. After hydrogen charging, the surface hydrogen concentrations between and within particular samples differed. This lack of uniformity may

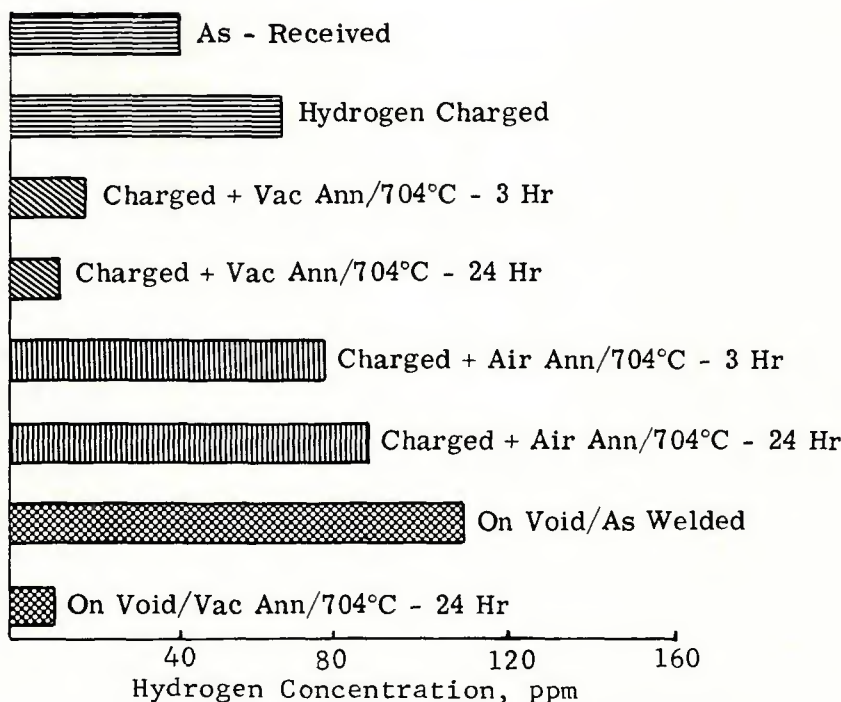


Fig. 13 — Summary of hydrogen concentration as a function of material processing

be responsible for anomalous behavior following this treatment.

4. Vacuum annealing at 704 C (1300 F) was found most significant in reducing the existing hydrogen concentration. Diffusion of hydrogen from a depth of 19 mm (0.750 in.) below the evacuated surface is not complete after 3 hr but is substantially complete after 24 hr. Vacuum annealing also eliminated hydrogen from the area of existing voids. Good agreement was found between calculated diffusion profiles and these experimental results.

5. Air annealing at 704 C (1300 F) was found to increase the existing hydrogen concentration. This is expected for samples with initial hydrogen concentrations less than 100-150 ppm.

## Acknowledgments

We wish to acknowledge the help of G. Hendry of the Grumman Materials and Processes Department, who participated in the selection, supply, and preparation of most of the specimens and to F. Federico of the Grumman Quality Control Laboratory for conducting the vacuum fusion bulk analyses. Our thanks also go to Dr. G. Geschwind and W. Aubin who helped in formulating the selection of samples and in reviewing this work.

## References

1. Wada, T., *Weld. Res. Abroad*, 13, 2, pp. 13-19, 1967.
2. Masubuchi, K., "Investigation of NASA-Sponsored Studies on Aluminum Welding," Contract No. NAS 8-24364, June 30, 1971.
3. Evans, R., "Porosity in Titanium Welds," DMIC Memorandum 194, Battelle Memorial Inst., Columbus, Ohio, 1964.
4. Mitchell, D., *Weld. J.*, 44, pp. 157-187s, 1965.
5. D'Andrea, M., *Weld. J.*, 45, pp. 178-187s, 1966.
6. Padawer, G. and Schneid, E., *The Lithium Microprobe as a Tool for Hydrogen Microanalysis at Surfaces*, Grumman Research Department Memorandum RM-467J, December 1969.
7. Padawer, G., Larson, D., Jr., and Adler, P., *Met. Trans.*, Vol. 2, p. 2287, 1971.
8. Tiner, N., Mackay, T., Asunmoa, S., and Ingersoll, R., *ASM Trans. Quart.*, Vol. 61, p. 195, 1968.
9. Toy, S. and Phillips, A., *Corrosion*, Vol. 26, p. 200, 1970.
10. Das, K. and Strobel, W., Boeing Co. Report in Ref. 2.
11. Barrington, A., Herzog, R., and Poschenrieder, W., "The Ion Microprobe Mass Spectrometer," *Prog. in Nuc. Energy Series IX, Analytical Chem.*, Vol. 7, Pergamon Press, New York, 1966.
12. Herzog, R., Poschenrieder, W., and Satkiewicz, F., *Mass Spectrometer Analysis of Solid Materials with the Ion-Microprobe Sputter Source*, NASA Report CR-683, January 1967.
13. Satkiewicz, F., *Sputter-Ion Source Mass Spectrometer Studies of Thin Films*, Technical Report AFAL-TR-69-332, 1970, Air Force Avionics Laboratory, WPAFB, Ohio.
14. Livanov, V., Bukhanova, A., and Kolachev, B., *Hydrogen in Titanium*, p. 94, D. Davey & Co., New York, 1965.
15. Crank, J., *The Mathematics of Diffusion*, p. 86, Oxford University Press, London, 1957.
16. Wasilewski, R. and Kehl, G., *Metallurgia*, Vol. 50, p. 225, 1954.
17. *Handbook of Chemistry and Physics*, 31st Edition, p. 2677, Chemical Rubber Publishing Company, Cleveland, Ohio, 1949.